3-2014

Spin Transfer of Quantum Information between Majorana Modes and a Resonator

Alexey Kovalev
University of Nebraska - Lncoln, alexey.kovalev@unl.edu

Amrit De
University of California, Riverside, amritde@gmail.com

Kirill Shtengel
University of California, Riverside, kirill.shtengel@ucr.edu

Spin Transfer of Quantum Information between Majorana Modes and a Resonator

Alexey A. Kovalev,[1] Amrit De,[2] and Kirill Shtengel[2]

[1]*Department of Physics and Astronomy and Nebraska Center for Materials and Nanoscience, University of Nebraska,
Lincoln, Nebraska 68588, USA*
[2]*Department of Physics and Astronomy, University of California, Riverside, California 92521, USA*

We show that resonant coupling and entanglement between a mechanical resonator and Majorana bound states can be achieved via spin currents in a 1D quantum wire with strong spin-orbit interactions. The bound states induced by vibrating and stationary magnets can hybridize, thus resulting in spin-current induced 4π-periodic torques, as a function of the relative field angle, acting on the resonator. We study the feasibility of detecting and manipulating Majorana bound states with the use of magnetic resonance force microscopy techniques.

Introduction.—Majorana zero states bound to domain walls in 1D and quasi-1D systems such as *p*-wave superconducting wires [1], edges of 2D topological insulators [2,3], and semiconducting quantum wires with strong spin-orbit interactions [4,5] can potentially be utilized to form nonlocal qubits, thus providing a platform for topological quantum computing [6–8]. Of these systems, spin-orbit-coupled semiconductor wires with proximity-induced superconductivity are of particular practical interest, with a number of recent experiments aiming at establishing the existence of Majorana bound states (MBS) there [9–12]. While further studies are needed to unambiguously confirm their existence [13–18], there is also an underlying need to further develop efficient techniques to manipulate MBS [19–25]. Several recent proposals suggested controlling topological qubits by coupling them to more conventional ones, such as flux qubits via the Aharonov-Casher effect [26–30].

Proposed experiments to observe MBS quite often rely on tunneling and transport effects that are indicative of the zero energy nature of these modes [13–18]. Some recent proposals are also related to unconventional Josephson effect in Majorana quantum wires and topological insulator (TI) edges where the periodicity is equal to 4π [1,4,31,32]. A dual effect whereby a torque between magnets exhibits 4π periodicity in the field orientations has also been suggested [33–35]. In this Letter, we show that it is precisely this effect that enables quantum information transfer between MBS and a mechanical resonator.

The idea of coupling a two-level system to vibrational modes to form a hybrid quantum system (a mechanical analog of cavity electrodynamics) has been successfully used in quantum optics [36] and in the field of nanomechanical resonators where a single phonon control has been demonstrated [37]. State-of-the-art nanomechanical resonators have high quality factors and can couple to a wide range of forces (e.g., produced by spin states of

localized atom-like systems); thus, they can serve as intermediary for coupling of quantum systems [38–40] and even for realizations of many-body simulators [41]. Quite excitingly, these developments can now make it possible to observe similar strong coupling effects in the context of topological qubits. However, how this can be achieved in the case of MBS is an open question, which we address in this Letter. In addition, this mechanism can be used to couple Majorana qubits to nontopological qubits such as nitrogen-vacancy centers [42]. Conservation of angular momentum in macrospin molecules can result in quantum entanglement of a tunneling spin with mechanical modes [43,44]. A flow of spin current between two magnets leads to spin-transfer torque effect [45,46] and mechanical torques [47,48], also by conservation of angular momentum.

In this Letter, we show that resonant coupling between a Majorana qubit and a mechanical resonator can be induced by spin currents flowing over portions (region of length ℓ_n in Fig. 1) of 1D semiconductor wire. The coupling
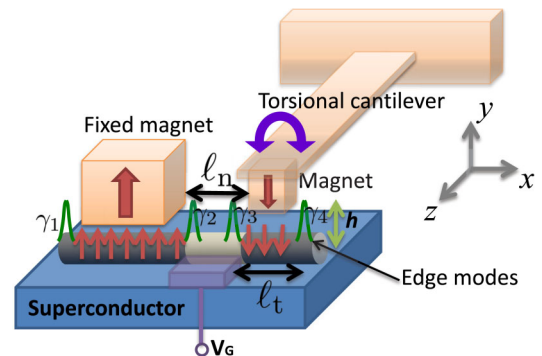

FIG. 1 (color online). A 1D semiconductor wire with strong spin-orbit coupling is placed on top of an *s*-wave superconductor. Majorana bound states are defined by magnetic fields of two magnets, one of which is free to vibrate. The gate V_G can be used to control their hybridization.

is controlled by nondissipative spin currents in a spin-transistor-type architecture [49]—which effectively allows or disallows the hybridization of two MBS. A nanomagnet attached to the resonator then feels the hybridization as a mechanical torque, which can result in the state transfer between the Majorana qubit and the mechanical resonator.

A Majorana qubit is formed by four MBS where three of these MBS are hybridized (Fig. 1). The nontopological region is formed by magnets with sharp field profiles and/or by heterojunction nanowires with contrasting g factors. In the following, we show that MBS are described by the effective low energy Hamiltonian $\mathcal{H} = iE^n(\theta)\gamma_2\gamma_3 + iE^t\gamma_3\gamma_4$, where θ is the angle between the magnetic fields, $E^{t(n)}$ describes the hybridization energy, and γ_i describe MBS. It is the θ dependence of the hybridization energy that leads to three interrelated effects: (i) coupling of the rotation of the magnet to the internal state of Majorana qubit, (ii) mechanical torque acting on the magnets, and (iii) spin current $j_s^z(x) = \text{Re}[\Psi^\dagger(x)\hat{\sigma}^z\hat{v}\Psi(x)]$ defined in the nontopological middle section in which the magnetic field is absent; here, the velocity operator is $\hat{v} = \partial\hat{H}/\partial p$. We find that the torque on the magnets [33–35] is generated solely by the spin current passing through the middle nontopological region when there is no hybridization over the topological regions in Fig. 1.

According to our theory, strong coupling between the Majorana qubit and the mechanical resonator can lead to a shift in the mechanical resonant frequency, Rabi oscillations, coherent state transfer, and entanglement. All of these effects could signify the presence of a Majorana qubit.

Spin currents and edge hybridization.—We consider a semiconductor wire with strong spin-orbit coupling in the presence of a Zeeman field (note that a TI edge gives qualitatively similar results). The wire is proximity coupled to an *s*-wave superconductor which induces the pairing strength Δ in the wire. A topological region is induced by external magnets (Fig. 1) where one of the magnets is attached to a mechanical resonator and can mechanically vibrate at frequency $\omega_r \ll \Delta$.

The 1D wire is described by a Bogoliubov–de Gennes Hamiltonian:

$$\hat{H} = \frac{p^2}{2m^*}\hat{\tau}^z + \frac{\alpha_{\text{so}}}{\hbar}p\hat{\tau}^z\hat{\sigma}^z - \mu\hat{\tau}^z + \Delta(\cos\phi\hat{\tau}^x - \sin\phi\hat{\tau}^y)$$
$$- b\hat{\sigma}^z + B(\cos\theta\hat{\sigma}^x - \sin\theta\hat{\sigma}^y), \qquad (1)$$

where m^* is the effective mass, α_{so} is the strength of the spin-orbit interaction, μ is the chemical potential, $\Delta e^{i\phi}$ is the superconducting pairing, b is the magnetic field along the z direction, and B is the magnetic field in the xy plane. Here, we use the Nambu spinor basis $\Psi^T = (\psi_\uparrow, \psi_\downarrow, \psi_\downarrow^\dagger, -\psi_\uparrow^\dagger)$, and the Pauli matrices $\hat{\sigma}^i$ and $\hat{\tau}^i$ describe spin and particle-hole sectors, respectively.

The Hamiltonian (1) supports both gapped and gapless phases; the transition between them can be driven by the Zeeman term [50,51]. The phase diagram is more complicated compared to a similar TI edge system [33,35] for which the $p^2\tau^z$ term is absent. Here we restrict ourselves to the case $\Delta^2 > b^2$ so that the Hamiltonian (1) describes two gapped phases: topological (*T*) if $\Delta^2 - b^2 < B^2 - \mu^2$ and nontopological (*N*) if $\Delta^2 - b^2 > B^2 - \mu^2$, separated by a quantum phase transition at $\Delta^2 - b^2 = B^2 - \mu^2$.

We analytically study the hybridization of the edge modes which results in spin currents and torques in *N-T-N* and *T-N-T* setups where a finite topological (*T*) or nontopological (*N*) region is created in an infinite semiconductor wire of the opposite kind (see Fig. 2). We assume that the phase of the superconducting pairing is constant throughout the wire, the magnetic field is always zero for *N* regions, and $b = 0$ in all regions. Then the gapped regions are described by parameters $\{\Delta, B, \mu, \theta\}$ for a *T* region and by $\{\Delta, \mu\}$ for an *N* region (see Fig. 2). We first determine the bound state at a single *T-N* boundary by finding a 4-component zero energy solution to the Hamiltonian (1) in the form $\Psi(x) = e^{\kappa x}\Psi(\kappa)$. We arrive at four solutions that decay into the topological region, i.e., with $\text{Re}(\kappa) > 0$, and four solutions that decay into the nontopological region, i.e., with $\text{Re}(\kappa) < 0$. A linear combination of these solutions on each side has to be continuous and have a continuous derivative at the boundary between *T* and *N* regions leading to a unique solution for MBS. We denote such normalized solutions as $|\psi_L\rangle$ for the left Majorana and as $|\psi_R\rangle$ for the right Majorana in Fig. 2. We use the lowest order perturbation theory to find the hybridization energy of the MBS provided that the normalized solutions for the left and right edges weakly overlap, i.e., $E^{n(t)} \approx |\langle\psi_L|H|\psi_R\rangle|$, where the index stands for the hybridization energy over the nontopological (topological) region. For the *T-N-T* system in Fig. 2, we obtain the hybridization energy over the nontopological region:

$$\frac{E^n}{E_0^n} \approx e^{-\ell_n\text{Re}(\kappa_2^n)}\cos\left[\frac{\theta}{2} + \Phi_0 + \ell_n\text{Im}(\kappa_2^n)\right]. \qquad (2)$$

Here, $\kappa_2^n = m^*/\hbar^2[i\alpha_{\text{so}} - i\sqrt{2(i\Delta + \mu)\hbar^2/m^* + \alpha_{\text{so}}^2}]$, $\theta = \theta_r - \theta_l$, and E_0^n and Φ_0 depend on parameters of the
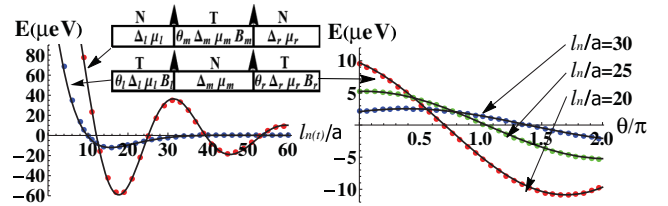

FIG. 2 (color online). Hybridization energies of two Majorana bound states over topological and nontopological regions in a semiconductor wire as a function of the hybridization region length (left) and relative angle of magnetic fields $\theta = \theta_r - \theta_l$ (right), only for *T-N-T* structures. The circles represent numerical results.

T and N regions and do not depend on ℓ_n and θ [52]. The spin current is

$$j_s^z = \frac{\partial E^n(\theta)}{\partial \theta}, \qquad (3)$$

which shows that the torque $\partial E^n(\theta)/\partial \theta$ on the magnets in Fig. 1 is generated by the spin current in the middle N region [52]. For the N-T-N system in Fig. 2, we obtain the hybridization energy over the topological region:

$$\frac{E^t}{E_0^t} \approx e^{-\ell_t \kappa_2^t} + |A_0| e^{-\ell_t \mathrm{Re}(\kappa_1^t)} \cos[\arg A_0 + \ell_t \mathrm{Im}(\kappa_1^t)], \quad (4)$$

where κ_1^t and κ_2^t are solutions of equation $\sqrt{B^2 - [\kappa^2 \hbar^2/2m + \mu]^2} = \Delta + \alpha_{so}\kappa$ satisfying the condition $\mathrm{Re}(\kappa) > 0$, and E_0^t and A_0 depend on parameters of the T and N regions and do not depend on ℓ_t and θ [52]. Figure 2 shows the hybridization energies given by Eqs. (2) and (4) for parameters corresponding to an InSb nanowire. We observe an exponential decay with separation and a 4π-periodic behavior with the relative angle of magnetic fields, which is typical for TI edges [33,35]. In addition, we find oscillatory behavior as a function of separation between the MBS suggested earlier [53,54]; however, we also obtain an additional exponentially decaying term and a phase shift in Eq. (4) which might be important for short T regions with asymmetric parameters. Furthermore, we find that these oscillations persist over a nontopological region (e.g., in the regime of a fully depleted electron band the oscillations are absent [55]). A possibility of MBS hybridization through virtual quasiparticle states [56] has not been taken into account as it can be suppressed by geometry and material engineering [56].

Numerical results for the static regime.—We map the Bogoliubov–de Gennes Hamiltonian (1) to a tight-binding model:

$$H = \sum_{i,\sigma,\sigma'} \left[c_{i+1\sigma}^\dagger \left(-t_0 \hat{\sigma}^0 + i\frac{\alpha_i}{2}\hat{\sigma}^z \right)_{\sigma\sigma'} c_{i\sigma'} + \mathrm{H.c.} \right]$$
$$+ \sum_{i,\sigma} (2t_0 - \mu_i) c_{i\sigma}^\dagger c_{i\sigma} + \sum_i (\tilde{\Delta}_i c_{i\uparrow}^\dagger c_{i\downarrow}^\dagger + \mathrm{H.c.})$$
$$+ \sum_i (\tilde{B}_i c_{i\uparrow}^\dagger c_{i\downarrow} + \mathrm{H.c.}), \qquad (5)$$

where $\hat{\sigma}^0$ is the identity matrix and we introduce complex parameters $\tilde{\Delta} = \Delta e^{i\phi}$ and $\tilde{B} = B e^{i\theta}$. In the long wavelength limit, the tight-binding model in Eq. (5) can be reduced to Eq. (1) with $t_0 = \hbar^2/2m^* a^2$, $\alpha = \alpha_{so}/a$, where a is the lattice constant. For Fig. 2, we use parameters consistent with setups based on InSb quantum wires [9], i.e., $m^* = 0.015 m_e$, $\alpha_{so} = 0.2$ eV Å, $a = 15$ nm, $\Delta = 0.5$ meV, and $g\mu_B = 1.5$ meV/T. We used a total of 500 grid sites for calculations. Results of numerical diagonalization of Hamiltonian (5) are shown in Fig. 2.

We observe near perfect agreement with the analytical Eqs. (2) and (4) when T regions are formed by uniform magnetic fields.

Next, in Figs. 3(a) and 3(b) we study the hybridization of MBS due to the modulation of the g factors (by a factor of ~ 30) in a GaSb-GaAs-GaSb nanowire heterostructures [57–59]. Such systems can partially or completely (when no coupling to the resonator is needed) relax the requirement for the sharpness of field profiles. Because of the conduction band mismatch, in this type-II quantum well, a finite gate voltage is necessary in order to hybridize MBS. The effects of nonuniform magnetic fields are closely examined in Fig. 3(c) where the wire is subjected to a constant magnetic field on one half and a field of magnetic dipole. The dipole is oriented as shown in Fig. 1 and is placed 1 μm from the center of the wire along x and at a height of h along the y axis. Somewhat sharper MBS are formed in Fig. 3(d) when instead of a dipole we consider a perpendicularly magnetized thin disk, which we approximate as a current loop of radius $R = 100$ nm with its center coinciding with the position of a dipole. The disk is placed at a height of h from the wire and its off-axis magnetic field decay implies that $\ell_n \gtrsim h$ for coupling between magnets to occur.

Dissipative dynamics.—We suppose that the section of the wire separating MBS γ_1 and γ_2 is sufficiently long (see Fig. 1). As follows from the previous discussion, the effective low energy theory for coupled dynamics of MBS and a mechanical resonator can be described to the lowest order by the Hamiltonian:
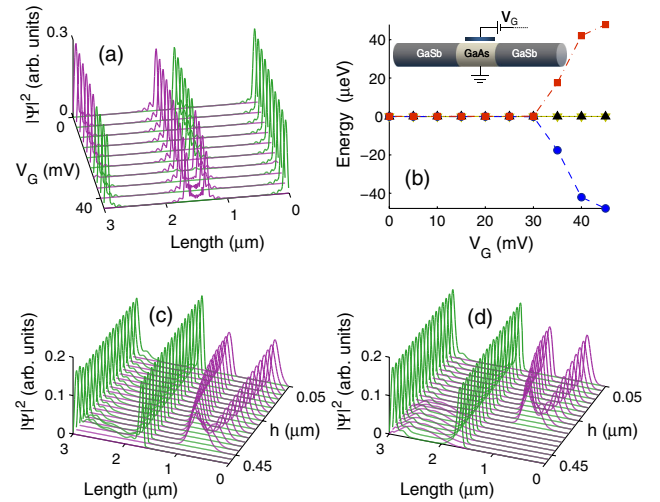

FIG. 3 (color online).   (a) We plot edge modes as a function of position and heterojunction bias voltage V_G, and (b) the corresponding energies as a function of V_G. We see hybridization at $V_G = 30$ meV. (c) The wire is subjected to a constant magnetic field on one half and a field of magnetic dipole at distance h on the other half. (d) The same as (c) but for a magnetic disk of radius $R = 100$ nm instead of dipole. In this figure we have used 300 grid sites with $a = 10$ nm.

$$\mathcal{H} = \hbar\omega_r a^\dagger a + iE^n(\theta)\gamma_2\gamma_3 + iE^t\gamma_3\gamma_4, \qquad (6)$$

where a is the annihilation operator of the resonant torsional mode of the cantilever so that $\theta = \theta_0 + \theta_{\mathrm{zpf}}(a^\dagger + a)$ with $\theta_{\mathrm{zpf}} = (\hbar^2/KI)^{1/4}$ being the angle of zero point fluctuations of the cantilever, K is the spring constant, I is the moment of inertia, $E^{n(t)}$ describes the hybridization energy in Eqs. (2) and (4), and γ_i describes MBS. Without loss of generality, we assume an odd electron parity in the wire, which defines the available Hilbert space of two fermions $b_1 = (\gamma_1 + i\gamma_2)/2$ and $b_2 = (\gamma_3 + i\gamma_4)/2$, i.e., $\alpha|1,0\rangle + \beta|0,1\rangle$ [60]. By rewriting Eq. (6) through fermionic operators b_1 and b_2, and expanding energies around θ_0, we arrive at the matrix Hamiltonian:

$$\mathcal{H} = \hbar\omega_r a^\dagger a + \left[E^n(\theta_0) + \frac{\partial E^n}{\partial \theta}\theta_{\mathrm{zpf}}(a^\dagger + a)\right]\hat{\sigma}^x + E^t\hat{\sigma}^z, \qquad (7)$$

where the Pauli operators act in the $|1,0\rangle$ and $|0,1\rangle$ basis. By tuning either $E^n(\theta_0)$ or E^t to coincide with $\hbar\omega_r/2$ (see Fig. 2), we can achieve different regimes of Rabi oscillations. Note that when $\langle\psi_L|H|\psi_R\rangle$ is not pure imaginary we recover additional terms proportional to σ^y in Eq. (7). Here, we analyze the case in which $\hbar\omega_r = 2E^t$ and $E^n(\theta_0) = 0$. From Eq. (2), the coupling strength (Rabi oscillations frequency) is

$$\mathfrak{g} = \frac{1}{2}\theta_{\mathrm{zpf}}E_0^n e^{-\ell_n \mathrm{Re}(\kappa_2^n)}. \qquad (8)$$

By taking smaller ℓ_n we can increase the coupling strength. The strong coupling regime is realized when $\omega_r/Q < \mathfrak{g}$, where Q is the quality factor of the cantilever. A pendulum based on single-walled carbon nanotube with an attached magnet of the size $60 \times 40 \times 20$ nm^3 can have $K = 3 \times 10^{-18}$ N m per radian and $I = 4 \times 10^{-34}$ kg m^2 [61]. If we take the corresponding $\theta_{\mathrm{zpf}} = 5 \times 10^{-5}$, $\omega_r = 5$ MHz, $E_0^n = 0.2$ meV, and $\ell_n = 300$ nm (see Fig. 2), we obtain $\mathfrak{g} = 400$ kHz, which is a strong coupling; e.g., a resonator with $\omega_r = 5$ MHz will have to have $Q > 12.5$ in order to be in the strong coupling regime. In order to switch off interactions between the Majorana qubit and the resonator, one can use special ℓ_t points at which the hybridization energy is close to zero (see Fig. 2). In principle, ℓ_t can be controlled by electrostatic gates [19] or supercurrents [25]. Note that the Majorana qubit is not topologically protected when controlled in this manner. This is, however, expected since for the realization of a universal set of quantum gates, some removal of topological protection would be necessary.

The time-dependent dissipative dynamics of the Hamiltonian (7) can be adequately simulated using the Lindblad master equation [62]:

$$\dot{\rho}(t) = -\frac{i}{\hbar}[\mathcal{H}(t),\rho] + \frac{1}{2}\sum_k [\mathcal{L}_k,\rho(t)\mathcal{L}_k^\dagger] + [\mathcal{L}_k\rho(t),\mathcal{L}_k^\dagger], \qquad (9)$$

where we assume that all requirements on the environment for the validity of this approximation apply. Here, $\mathcal{L}_k$ are the Lindblad operators, $\mathcal{L}_1 = \sqrt{1/T_1}\sigma_-$ and $\mathcal{L}_2 = \sqrt{1/T_\varphi}\sigma_+\sigma_-$ correspond to the Majorana qubit coupling to the environment, and $\mathcal{L}_3 = \sqrt{(\bar{n}_r + 1)\omega_r/Q}a$ and $\mathcal{L}_4 = \sqrt{\bar{n}_r\omega_r/Q}a^\dagger$ correspond to the dissipation of the resonator where $\bar{n}_r = [\exp(\omega_r/k_B T) - 1]^{-1}$. The qubit's lifetimes are given by T_1 and $1/T_2 = 1/2T_1 + 1/T_\varphi$. The Majorana qubit can decohere due to tunneling of fermions in the presence of an external environment such as phonons, two-level systems, classical noise [63], as well as quasiparticle poisoning [64] and noisy gates [65]. As T_1 and T_2 times can strongly depend on the concrete realization, in our analysis we choose decoherence times that are consistent with the abovementioned mechanisms $T_1 = 70$ μs, $T_2 = 90$ μs).

We present numerical solutions of Eq. (9) for different resonator quality factors, i.e., for $Q = 10^6$ in Figs. 4(a) and 4(b) and for $Q = 10^5$ in Figs. 4(c) and 4(d). As the initial state, we assume the product state of the qubit and the resonator at temperature $T = 10$ mK corresponding to the occupation number $\bar{n}_r = 0.26$, e.g., as a result of sideband cooling [66]. Dotted lines represent the Rabi oscillations while the bold lines represent the process in which the Majorana qubit is repeatedly tuned in and out of resonance with the resonator. In such a process the qubit state is transferred from the qubit to the resonator, then stored in
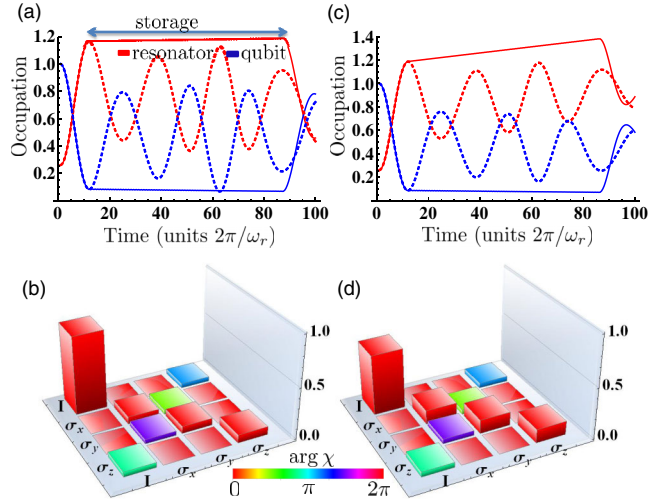

FIG. 4 (color online). (a) Rabi oscillations of a Majorana qubit coupled to a mechanical resonator. The qubit's initial state is $|0,1\rangle$ in Eq. (7). (b) The quantum process tomography of a process in which qubit state is transferred to the resonator, then stored in the resonator while the systems are detuned, and finally transferred back to the qubit. (c),(d) Same as (a) and (b) but for a resonator with smaller quality factor.

the resonator while the systems are detuned, and finally transferred back to the qubit. We can completely describe the storage process by quantum process tomography in which the final density matrix of the qubit $\hat{\rho}_{out}$ is described by the 4×4 process matrix $\hat{\chi}$, such that $\hat{\rho}_{out} = \sum \chi_{i,j} \hat{\sigma}^i \hat{\rho}_{in} \hat{\sigma}^j$; here, $\hat{\rho}_{in}$ is the initial density matrix of the qubit. In Figs. 4(b) and 4(d) we plot the matrix $\hat{\chi}$ where the two plots correspond to fidelities $F = \chi_{1,1} = 78\%$ and $F = \chi_{1,1} = 60\%$, respectively.

Conclusions.—We demonstrated spin-current mediated resonant coupling between a Majorana qubit and a mechanical resonator. The coupling can manifest itself in a shift of the mechanical resonant frequency, Rabi oscillations, coherent state transfer, and Majorana qubit-resonator entanglement. In addition, the spin-current mediated coupling can facilitate both control of Majorana zero modes in a quantum wire and transfer of quantum information between topological and conventional qubits. The possibility to control the coupling and nondissipative spin currents in the spin-transistor-type architecture paves the way for applications in novel electronic devices. Our predictions can be tested by employing the magnetic resonance force microscopy techniques.

[1] A. Y. Kitaev, Phys. Usp. **44**, 131 (2001).
[2] L. Fu and C. L. Kane, Phys. Rev. Lett. **100**, 096407 (2008).
[3] J. Nilsson, A. R. Akhmerov, and C. W. J. Beenakker, Phys. Rev. Lett. **101**, 120403 (2008).
[4] R. M. Lutchyn, J. D. Sau, and S. Das Sarma, Phys. Rev. Lett. **105**, 077001 (2010).
[5] Y. Oreg, G. Refael, and F. von Oppen, Phys. Rev. Lett. **105**, 177002 (2010).
[6] C. Nayak, S. H. Simon, A. Stern, M. Freedman, and S. Das Sarma, Rev. Mod. Phys. **80**, 1083 (2008).
[7] J. Alicea, Rep. Prog. Phys. **75**, 076501 (2012).
[8] C. Beenakker, Annu. Rev. Condens. Matter Phys. **4**, 113 (2013).
[9] V. Mourik, K. Zuo, S. M. Frolov, S. R. Plissard, E. P. A. M. Bakkers, and L. P. Kouwenhoven, Science **336**, 1003 (2012).
[10] M. T. Deng, C. L. Yu, G. Y. Huang, M. Larsson, P. Caroff, and H. Q. Xu, Nano Lett. **12**, 6414 (2012).
[11] A. Das, Y. Ronen, Y. Most, Y. Oreg, M. Heiblum, and H. Shtrikman, Nat. Phys. **8**, 887 (2012).
[12] L. P. Rokhinson, X. Liu, and J. K. Furdyna, Nat. Phys. **8**, 795 (2012).
[13] D. Bagrets and A. Altland, Phys. Rev. Lett. **109**, 227005 (2012).
[14] J. Liu, A. C. Potter, K. T. Law, and P. A. Lee, Phys. Rev. Lett. **109**, 267002 (2012).
[15] D. I. Pikulin, J. P. Dahlhaus, M. Wimmer, H. Schomerus, and C. W. J. Beenakker, New J. Phys. **14**, 125011 (2012).
[16] E. J. H. Lee, X. Jiang, R. Aguado, G. Katsaros, C. M. Lieber, and S. De Franceschi, Phys. Rev. Lett. **109**, 186802 (2012).
[17] S. Das Sarma, J. D. Sau, and T. D. Stanescu, Phys. Rev. B **86**, 220506 (2012).
[18] A. D. K. Finck, D. J. Van Harlingen, P. K. Mohseni, K. Jung, and X. Li, Phys. Rev. Lett. **110**, 126406 (2013).
[19] J. Alicea, Y. Oreg, G. Refael, F. von Oppen, and M. P. A. Fisher, Nat. Phys. **7**, 412 (2011).
[20] J. C. Y. Teo and C. L. Kane, Phys. Rev. Lett. **104**, 046401 (2010).
[21] J. D. Sau, S. Tewari, and S. Das Sarma, Phys. Rev. A **82**, 052322 (2010).
[22] J. D. Sau, D. J. Clarke, and S. Tewari, Phys. Rev. B **84**, 094505 (2011).
[23] K. Flensberg, Phys. Rev. Lett. **106**, 090503 (2011).
[24] B. I. Halperin, Y. Oreg, A. Stern, G. Refael, J. Alicea, and F. von Oppen, Phys. Rev. B **85**, 144501 (2012).
[25] A. Romito, J. Alicea, G. Refael, and F. von Oppen, Phys. Rev. B **85**, 020502 (2012).
[26] F. Hassler, A. R. Akhmerov, C.-Y. Hou, and C. W. J. Beenakker, New J. Phys. **12**, 125002 (2010).
[27] L. Jiang, C. L. Kane, and J. Preskill, Phys. Rev. Lett. **106**, 130504 (2011).
[28] P. Bonderson and R. M. Lutchyn, Phys. Rev. Lett. **106**, 130505 (2011).
[29] F. Hassler, A. R. Akhmerov, and C. W. J. Beenakker, New J. Phys. **13**, 095004 (2011).
[30] D. Pekker, C.-Y. Hou, V. E. Manucharyan, and E. Demler, Phys. Rev. Lett. **111**, 107007 (2013).
[31] L. Fu and C. L. Kane, Phys. Rev. B **79**, 161408 (2009).
[32] L. Jiang, D. Pekker, J. Alicea, G. Refael, Y. Oreg, and F. von Oppen, Phys. Rev. Lett. **107**, 236401 (2011).
[33] Q. Meng, V. Shivamoggi, T. L. Hughes, M. J. Gilbert, and S. Vishveshwara, Phys. Rev. B **86**, 165110 (2012).
[34] P. Kotetes, G. Schön, and A. Shnirman, J. Korean Phys. Soc. **62**, 1558 (2013).
[35] L. Jiang, D. Pekker, J. Alicea, G. Refael, Y. Oreg, A. Brataas, and F. von Oppen, Phys. Rev. B **87**, 075438 (2013).
[36] S. Groblacher, K. Hammerer, M. R. Vanner, and M. Aspelmeyer, Nature (London) **460**, 724 (2009).
[37] O. D. O'Connell, M. Hofheinz, M. Ansmann, R. C. Bialczak, M. Lenander, E. Lucero, M. Neeley, D. Sank, H. Wang, M. Weides et al., Nature (London) **464**, 697 (2010).
[38] J. I. Cirac and P. Zoller, Phys. Rev. Lett. **74**, 4091 (1995).
[39] V. N. Smelyanskiy, A. G. Petukhov, and V. V. Osipov, Phys. Rev. B **72**, 081304 (2005).
[40] P. Rabl, P. Cappellaro, M. V. Gurudev Dutt, L. Jiang, J. R. Maze, and M. D. Lukin, Phys. Rev. B **79**, 041302 (2009).
[41] D. Porras and J. I. Cirac, Phys. Rev. Lett. **93**, 263602 (2004).
[42] S. Kolkowitz, A. C. Bleszynski Jayich, Q. P. Unterreithmeier, S. D. Bennett, P. Rabl, J. G. E. Harris, and M. D. Lukin, Science **335**, 1603 (2012).
[43] A. A. Kovalev, L. X. Hayden, G. E. W. Bauer, and Y. Tserkovnyak, Phys. Rev. Lett. **106**, 147203 (2011).

[44] D. A. Garanin and E. M. Chudnovsky, Phys. Rev. X **1**, 011005 (2011).

[45] L. Berger, Phys. Rev. B **54**, 9353 (1996).

[46] J. Slonczewski, J. Magn. Magn. Mater. **159**, L1 (1996).

[47] A. A. Kovalev, G. E. W. Bauer, and A. Brataas, Phys. Rev. B **75**, 014430 (2007).

[48] G. Zolfagharkhani, A. Gaidarzhy, P. Degiovanni, S. Kettemann, P. Fulde, and P. Mohanty, Nat. Nanotechnol. **3**, 720 (2008).

[49] S. Datta and B. Das, Appl. Phys. Lett. **56**, 665 (1990).

[50] M. Sato, Y. Takahashi, and S. Fujimoto, Phys. Rev. Lett. **103**, 020401 (2009).

[51] M. Sato and S. Fujimoto, Phys. Rev. B **79**, 094504 (2009).

[52] See Supplemental Material at http://link.aps.org/supplemental/10.1103/PhysRevLett.112.106402 for detailed expressions.

[53] S. Das Sarma, J. D. Sau, and T. D. Stanescu, Phys. Rev. B **86**, 220506 (2012).

[54] D. Rainis, L. Trifunovic, J. Klinovaja, and D. Loss, Phys. Rev. B **87**, 024515 (2013).

[55] J. D. Sau, S. Tewari, and S. Das Sarma, Phys. Rev. A **82**, 052322 (2010).

[56] A. A. Zyuzin, D. Rainis, J. Klinovaja, and D. Loss, Phys. Rev. Lett. **111**, 056802 (2013).

[57] Y. N. Guo, J. Zou, M. Paladugu, H. Wang, Q. Gao, H. H. Tan, and C. Jagadish, Appl. Phys. Lett. **89**, 231917 (2006).

[58] B. Ganjipour, H. A. Nilsson, B. M. Borg, L.-E. Wernersson, L. Samuelson, H. Q. Xu, and C. Thelander, Appl. Phys. Lett. **99**, 262104 (2011).

[59] A. De and C. E. Pryor, Phys. Rev. B **76**, 155321 (2007).

[60] Whether the fermion parity is even or odd is inconsequential for our discussion; what is important is that the parity does not fluctuate. The qubit decoherence rate associated with the stray quasiparticle tunneling in and out of the wire has been estimated to be no worse than ~10 MHz for the relevant range of parameters [64,67] and in practice can be made orders of magnitude slower than that [68,69].

[61] J. C. Meyer, M. Paillet, and S. Roth, Science **309**, 1539 (2005).

[62] J. Johansson, P. Nation, and F. Nori, Comput. Phys. Commun. **183**, 1760 (2012).

[63] G. Goldstein and C. Chamon, Phys. Rev. B **84**, 205109 (2011).

[64] D. Rainis and D. Loss, Phys. Rev. B **85**, 174533 (2012).

[65] M. J. Schmidt, D. Rainis, and D. Loss, Phys. Rev. B **86**, 085414 (2012).

[66] J. D. Teufel, T. Donner, D. Li, J. W. Harlow, M. S. Allman, K. Cicak, A. J. Sirois, J. D. Whittaker, K. W. Lehnert, and R. W. Simmonds, Nature (London) **475**, 359 (2011).

[67] F. J. Burnell, A. Shnirman, and Y. Oreg, Phys. Rev. B **88**, 224507 (2013).

[68] O.-P. Saira, A. Kemppinen, V. F. Maisi, and J. P. Pekola, Phys. Rev. B **85**, 012504 (2012).

[69] D. Riste, M. Dukalski, C. A. Watson, G. de Lange, M. J. Tiggelman, Y. M. Blanter, K. W. Lehnert, R. N. Schouten, and L. DiCarlo, Nature (London) **502**, 350 (2013).